Long-Lasting Molecular Orientation Induced by a Single Terahertz Pulse

Long Xu, Ilia Tutunnikov, Erez Gershnabel, Yehiam Prior, and Ilya Sh. Averbukh*
AMOS and Department of Chemical and Biological Physics, The Weizmann Institute of Science, Rehovot 7610001, Israel

(Received 10 March 2020; revised 10 May 2020; accepted 3 June 2020; published 1 July 2020)

We present a novel, previously unreported phenomenon appearing in a thermal gas of nonlinear polar molecules excited by a single THz pulse. We find that the induced orientation lasts long after the excitation pulse is over. In the case of symmetric-top molecules, the time-averaged orientation remains indefinitely constant, whereas in the case of asymmetric-top molecules the orientation persists for a long time after the end of the pulse. We discuss the underlying mechanism, study its nonmonotonous temperature and amplitude dependencies, and show that there exist optimal parameters for maximal residual orientation. The persistent orientation implies a long-lasting macroscopic dipole moment, which may be probed by even harmonic generation and may enable deflection by inhomogeneous electrostatic fields.

DOI: 10.1103/PhysRevLett.125.013201

Introduction.—Molecular alignment and orientation, mostly by ultrashort optical pulses, attract considerable interest owing to their extreme importance in a variety of applications in physics, chemical reaction dynamics, and attosecond electron dynamics (for reviews see, e.g., Refs. [1–5] and references therein). In recent years, advanced THz pulses [6] were utilized to orient polar linear molecules [7–9], and later on, symmetric- [10] and asymmetric-top molecules [11]. The pioneering theoretical studies of the hybrid excitation, combining THz and optical pulses [12–14], led to extended theoretical research [15–18] and finally resulted in an experimental demonstration of enhanced orientation [9]. In the most studied case of linear molecules, the induced orientation shows a short transient signal with periodic recurrences (quantum revivals [19–21]), all riding on zero baseline. This is consistent with the classical dynamics of a free linear rotor whose axis is confined to a plane of rotation perpendicular to the conserved vector of angular momentum. As a result, the time-averaged orientation signal is strictly zero.

In this Letter, we analyze the case of general molecular rotors, symmetric or asymmetric. The free evolution of their molecular axes is, in general, nonplanar, and the molecules perform precessionlike motion about the vector of angular momentum. We theoretically study the orientation of a gas of symmetric- and asymmetric-top molecules excited by a single linearly polarized THz pulse. The THz pulse not only induces a short time transient dipole signal (transient orientation), but also results in a steady molecular orientation that persists for a long time after the end of the pulse. In the case of symmetric-top molecules, the ensemble-averaged long-time orientation remains constant, while for asymmetric-top molecules, it persists on a time scale exceeding the duration of the pulse by several orders of magnitude. We show that this phenomenon is classical in nature and discuss its underlying mechanism. The degree of orientation is shown to have nonmonotonous temperature and amplitude dependencies.

Equations of motion.—The free motion of symmetric and asymmetric tops is a standard classical and quantum mechanical textbook topic, whereas the interaction with an external field complicates the problem considerably (see Refs. [22,23] and references therein). The Hamiltonian describing molecular rotation driven by an external time-dependent field interacting with the molecular dipole is given by [24] $H(t) = H_R + H_{\rm int}(t)$, where H_R is the rotational kinetic energy Hamiltonian and $H_{\rm int}(t) = -\boldsymbol{\mu}\cdot\mathbf{E}(t)$ is the molecular dipole-field interaction. The electric field of the THz pulse is modeled (Fig. 1) as $\mathbf{E}(t) = E_0(1-2\kappa t^2)e^{-\kappa t^2}\mathbf{e}_Z$ [25]. Here E_0 is the peak amplitude, κ determines the width of the pulse, and $\mathbf{e}_Z$ is the unit vector along the laboratory Z axis. In this work, we use parameters typical for currently available THz pulses [26–29]. We consider the problem both classically and quantum mechanically. For the quantum mechanical treatment, the wave function is expanded in the basis of free symmetric-top wave functions $|JKM\rangle$ [30]. Here J is the total angular momentum, while K

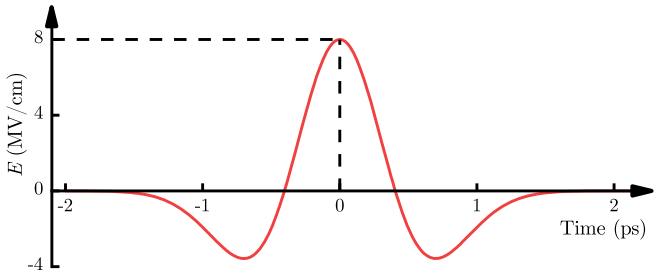

FIG. 1. Time-dependent field amplitude of the THz pulse defined by $E(t) = E_0(1-2\kappa t^2)e^{-\kappa t^2}$, where $E_0 = 8.0$ MV/cm and $\kappa = 3.06$ ps^{-2}. Note that the time integral of the electric field is identically zero.

and M denote its projections on the molecule-fixed axis and the laboratory-fixed Z axis, respectively. The time-dependent Schrödinger equation $i\hbar\partial_t|\Psi(t)\rangle = H(t)|\Psi(t)\rangle$ is solved by numerical exponentiation of the Hamiltonian matrix (see ExpoKit [31]). We average the orientation signal over the initial thermal state of the molecular rotor. In the case of symmetric-top molecules, the nuclear spin statistics [32] is taken into account. A detailed description of our scheme is presented in Sec. I of the Supplemental Material [33].

In the classical limit, the rotational motion of rigid molecules driven by external time-dependent fields was modeled with the help of Euler's equations [36]

$$\mathbf{I}\dot{\mathbf{\Omega}} = (\mathbf{I}\mathbf{\Omega}) \times \mathbf{\Omega} + \mathbf{T}, \tag{1}$$

where $\mathbf{I} = \mathrm{diag}(I_a, I_b, I_c)$ is the moment of inertia tensor ($I_a \le I_b \le I_c$), $\mathbf{\Omega} = (\Omega_a, \Omega_b, \Omega_c)$ is the angular velocity, and $\mathbf{T} = (T_a, T_b, T_c)$ is the external torque expressed in the molecular frame. The latter is given by $\mathbf{T} = \boldsymbol{\mu} \times Q\mathbf{E}$, where $\mathbf{E}$ is the external electric field defined in the laboratory frame, and Q is a 4×3 matrix composed of the elements of a quaternion [37,38]. A quaternion is defined as a quadruplet of real numbers, $q = (q_0, q_1, q_2, q_3)$ and it has a simple equation of motion $\dot{q} = q\Omega/2$, where $\Omega = (0, \mathbf{\Omega})$ is a pure quaternion and the quaternion multiplication rule is implied [37,38]. To simulate the behavior of a thermal ensemble, we use the Monte Carlo approach. For each molecule, we numerically solve the system of Euler's [Eq. (1)] and quaternion equations of motion. Our ensemble consists of $N = 10^7$ sample molecules and the initial uniform random quaternions were generated using the recipe from Ref. [39]. Initial molecular angular velocities were generated according to the Boltzmann distribution $f(\Omega_i) \propto \exp[-I_i\Omega_i^2/(2k_BT)]$, $i = a, b, c$, where T is the rotational temperature and k_B is the Boltzmann constant.

Simulation results.—In this Letter, we used methyl chloride (CH_3Cl) and propylene oxide (PPO, CH_3CHCH_2O) molecules, as typical examples of symmetric- and asymmetric-top molecules, respectively. Molecular parameters are provided in Sec. II of the Supplemental Material [33].

Figure 2 shows time-dependent ensemble-averaged projection of the dipole moment, $\langle\mu_Z\rangle(t)$ on the laboratory Z axis, along which the THz pulse is polarized. The angle brackets $\langle\cdots\rangle$ denote thermal averaging over the initial molecular state. The initial temperature is set to $T = 5$ K. The two other averaged projections of the molecular dipole, $\langle\mu_X\rangle(t)$ and $\langle\mu_Y\rangle(t)$ are zero, due to the axial symmetry of the system. On the short time scale (first $\approx$10 ps), the quantum results are in good agreement with the classical ones. Both symmetric [Fig. 2(a)] and asymmetric-top [Fig. 2(b)] molecules immediately respond to the THz pulse by a transient dipole signal. However, long after the pulse, the orientation does not completely disappear and a long-lasting persistent dipole signal remains (see insets of Fig. 2). This remarkable behavior is the main result of our Letter.

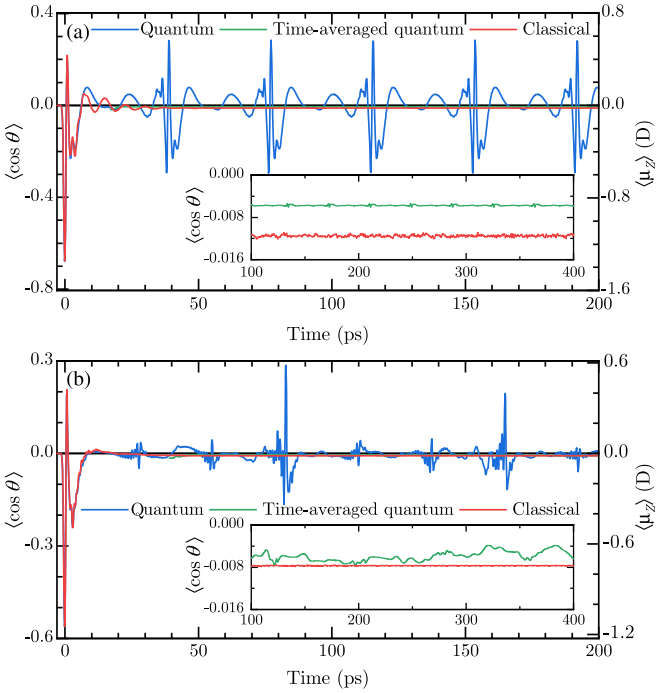

FIG. 2. Time-dependent orientation factor, $\langle\cos\theta\rangle$ or ensemble averaged Z projection of the dipole moment, $\langle\mu_Z\rangle$ as a function of time for (a) CH_3Cl and (b) PPO molecules. The results of the quantum and classical simulations are shown in blue and red lines, respectively. The green curve represents the sliding time average defined by $\overline{\langle\mu_Z\rangle}(t) = (\Delta t)^{-1}\int_{t-\Delta t/2}^{t+\Delta t/2} dt'\langle\mu_Z\rangle(t')$. Here Δt is selected to be approximately equal to revival period, (a) $\Delta t = 38.2$ ps, (b) $\Delta t = 82.2$ ps, respectively. The insets show a magnified portion of the signals.

In the classical limit, the long-lasting orientation of symmetric- and asymmetric-top molecules remains constant indefinitely (until the orientation is destroyed by collisions). Quantum simulations exhibit the expected quasiperiodic beats [19] due to quantum revivals, but a moving window average of the quantum results (see captions of Fig. 2) keeps close to the classically predicted constant orientation. In the case of symmetric-top molecules the time-averaged quantum signal is essentially constant [Fig. 2(a)]. In the case of asymmetric-top molecules [Fig. 2(b)], the time-averaged signal is long lasting (hundreds of ps in the present case), and on an even longer time scale, the absolute value of the orientation slowly decreases and eventually changes its sign (not shown). The difference between symmetric- and asymmetric-top molecules stems from the fact that quantum-mechanical states of the latter are nondegenerate and have different parity [30]. As a consequence, any state that is internally oriented at some point in time cannot be an eigenstate and will oscillate between being oriented and anti-oriented, an effect known as dynamical tunneling [40].

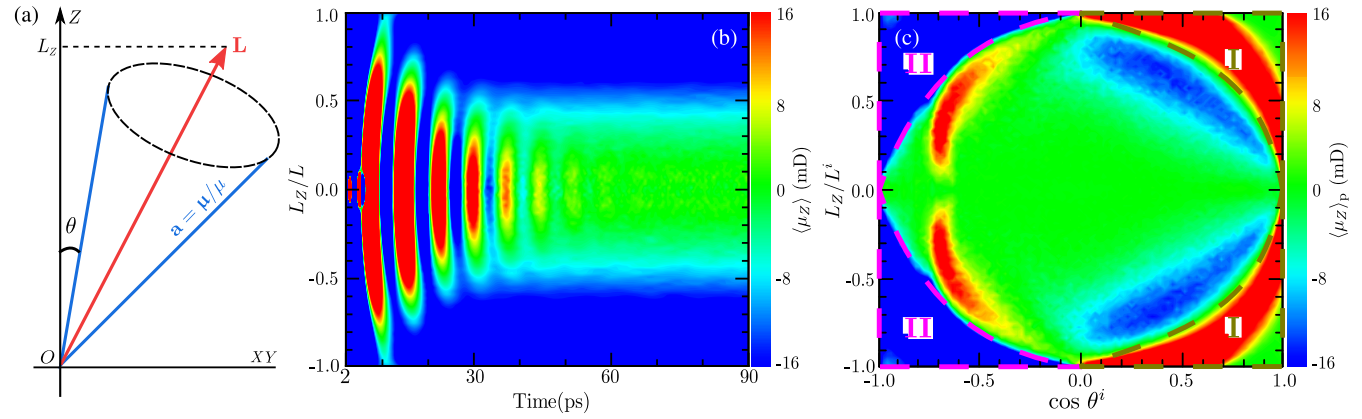

FIG. 3. Thermal ensemble of classical symmetric-top molecules excited by a Z-polarized THz pulse. (a) Illustration of the precession motion of the molecular symmetry axis $\mathbf{a}$ (in blue) about the angular momentum vector $\mathbf{L}$ (in red), θ is the polar angle between $\mathbf{a}$ ($\boldsymbol{\mu}$) and the Z axis. (b) The dipole signal $\langle \mu_Z \rangle$ as a function of time and L_Z/L. (c) Permanent value of $\langle \mu_Z \rangle_p$ after the pulse as a function of the initial conditions before the pulse: $\cos\theta^i$ and L_Z/L^i. Two regions, I and II, are marked in (c). The color scales in (b) and (c) are in the units of millidebye (mD).

Two additional factors should be mentioned: centrifugal distortion and radiation emission due to fast changes in the dipole moment. The centrifugal distortion leads to eventual decay of the periodic quantum revival peaks [10,41] due to the dephasing of the rotational states. However, the dipole signal averaged over multiple revival periods is hardly affected (see Sec. III of the Supplemental Material [33]). Fast variation of the dipole signal during each revival event may lead to radiative emission and gradual reduction of the rotational energy [10,41]. However, in the case of a rarified molecular gas considered here, the estimated relative energy loss during a single revival is negligible.

Recently, a related phenomenon of persistent orientation was reported [42,43], where laser pulses with twisted polarization were applied to chiral molecules. In the present work, however, we use a single unshaped THz pulse, chirality is not required and the underlying mechanism is different, as is discussed in the next section.

Qualitative discussion.—To understand the origin of the long-lasting orientation shown in Fig. 2, we first analyze the case of an ensemble of classical symmetric-top molecules excited by a Z-polarized THz pulse. The motion of free, prolate for definiteness, symmetric-top molecules is defined by a simple vectorial differential equation $\dot{\mathbf{a}} = (\mathbf{L}/I) \times \mathbf{a}$, where $\mathbf{a}$ is a unit vector along the molecular axis of symmetry, I is the moment of inertia ($I_a < I_b = I_c \equiv I$), and $\mathbf{L}$ is the vector of angular momentum. Explicit solution of this equation is provided in Sec. IV of the Supplemental Material [33]. Figure 3(a) shows the general motion of a symmetric top, namely precession of $\mathbf{a}$ about the vector $\mathbf{L}$ at rate L/I, where L is the magnitude of the angular momentum. The time-averaged projection of the dipole on the Z axis is given by

$$\overline{\mu_Z} = \mu \lim_{\tau\to\infty} \frac{1}{\tau} \int_0^\tau \mathbf{a}(t) \cdot \mathbf{e}_Z dt = \mu \frac{L_Z L_a}{L^2}, \tag{2}$$

where μ is the magnitude of the dipole and $\mathbf{e}_Z$ is a unit vector along the Z axis. The solution $\mathbf{a}(t)$ describes the field-free stage of the motion, therefore L_a and L in the above equation are taken at the end of the pulse. Notice that the projection of the angular momentum on the axis of the pulse, L_Z is a constant of motion. The projection, L_a of the angular momentum on the molecular symmetry axis can be expressed in terms of L_X, L_Y, L_Z, and the Euler angles [30]: $L_a = L_X \sin\theta\cos\phi + L_Y \sin\theta \sin\phi + L_Z \cos\theta$.

Thus, we have $\overline{\mu_Z}/\mu = (L_Z/L)^2 \cos\theta + (L_X L_Z/L^2) \times \sin\theta\cos\phi + (L_Y L_Z/L^2) \sin\theta \sin\phi$. Denoting $\cos\theta = x$ and $\cos\theta_1 = L_Z/L = y$, the ensemble averaged dipole moment is given by

$$\overline{\langle \mu_Z \rangle} \propto \mu \int_{-1}^{1} x P_0(x) dx, \tag{3}$$

where $P_0 \propto \int y^2 L^2 P_1(x, y, L) dL dy$ and $P_1(x, y, L)$ is the joint probability distribution of $\cos\theta$, $\cos\theta_1$ and L at the end of the pulse. Terms proportional to $\sin\phi$ and $\cos\phi$ in the expression for $\overline{\mu_Z}/\mu$ do not contribute to the average, because a THz pulse does not affect a uniform distribution of the angle ϕ. For initial temperature $T = 0$ K, $\overline{\mu_Z}$ vanishes because $L_Z \equiv 0$ before and after the pulse. Also, in the limit of a pulse of vanishing duration ($\kappa \to \infty$, see Fig. 1), the permanent orientation tends to zero because P_0 keeps the initial symmetric distribution just after the pulse. As an illustration, P_1 can be written down explicitly for a model system of thermalized symmetric-top molecules ($I/I_a = w > 1$) subject to a constant dc field of amplitude E_0 which is then abruptly switched off. In this case, $P_1(x, y, l) \propto f(x) g(y, l) = \exp(\epsilon x) \exp\{-l^2[1 + y^2(w-1)]\}$, where $\epsilon = \mu E_0/k_B T$ and $l = L/\sqrt{2 I k_B T}$ (see Sec. V of the Supplemental Material [33]). Clearly, $\overline{\langle \mu_Z \rangle} \neq 0$, because $\exp(\epsilon x)$ is not a symmetric function in the interval $x \in [-1, 1]$ for $\epsilon > 0$.

To explore the long-lasting orientation and to better understand its physical origin, we consider the underlying dynamics in more detail. After the end of the pulse, at $t > 2$ ps (see Fig. 1), the ratio L_Z/L is constant. Figure 3(b) shows the ensemble averaged dipole moment, $\langle \mu_Z \rangle$ in a three-dimensional color-coded plot, as a function of time and L_Z/L. Right after the pulse ($t = 2$ ps) approximately all the molecules have a negative Z projection of their dipoles. Moreover, at long time, molecules with $L_Z \simeq \pm L$ (upper and lower blue bands) contribute to the overall negative dipole signal, while for molecules with $|L_Z/L| \ll 1$ (central portion of the figure), the time-averaged dipole signal tends to zero. In the absence of external fields, the molecules with angular momentum along $\pm Z$ axis and the symmetry axis initially directed along $-Z$, will continue to precess around $-Z$ direction forever. In contrast, the contribution of molecules with angular momentum lying in the XY plane ($|L_Z/L| \ll 1$) averages to zero and they do not contribute to the long-lasting orientation. In the special case of initial temperature of $T = 0$ K, L_Z remains identically zero after the pulse (L_Z is conserved), thus forbidding the permanent orientation.

The physical origin of the permanent (negative) orientation observed in Fig. 3(b) can be further analyzed by considering it as a function of *the initial* orientation factor, $\cos\theta^i$ and the value of L_Z/L^i before the pulse. Figure 3(c) shows the value of $\langle \mu_Z \rangle$ taken after 100 ps [after the orientation settled to its permanent value, see Fig. 2(a)], denoted as $\langle \mu_Z \rangle_p$, as a function of the initial conditions. Angle θ^i is the initial angle between the dipole moment and Z axis [see Fig. 3(a)]. The figure shows that molecules with $|\cos\theta^i| \simeq 1$ and $L_Z/L^i = \pm 1$ (regions denoted by I and II, blue and red in the figure) maintain the nonzero permanent orientation, while the orientation of molecules in other regions tends to zero. To understand the reason for this, we consider molecules in each region separately and follow their time evolution in the presence of the THz pulse.

Initially, molecules in region I precess about the $+Z$ direction, because $L_Z \simeq \pm L^i$ and $\cos\theta^i \simeq 1$. During the first phase of the THz pulse, when the field points along $-Z$ (see Fig. 1), it tends to flip the molecular dipoles. In contrast, during the second phase, when the field is along $+Z$ (see Fig. 1), it pushes the dipoles towards $+Z$, thus facilitating the permanent orientation. Molecules in region II, which initially precess about $-Z$ ($L_Z \simeq \pm L^i$, $\cos\theta^i \simeq -1$) respond oppositely as compared to the molecules in region I. For the chosen parameters of the THz pulse (see Fig. 1), there is an imbalance between these two groups resulting in the excess of molecules precessing about $-Z$ axis. This leads to the overall negative permanent orientation.

The qualitative mechanism described above for the case of symmetric-top molecules is essentially the same for asymmetric-top molecules as well. Figure 4(a) depicts the permanent values of $\langle \mu_Z \rangle_p$ as a function of initial orientation quantified by $\cos\theta^i$ for the previously considered methyl chloride and propylene oxide molecules. In both cases, the THz pulse preferentially supports the molecular precession about the $-Z$ direction, as opposed to $+Z$, so that the overall long-time dipole value is negative.

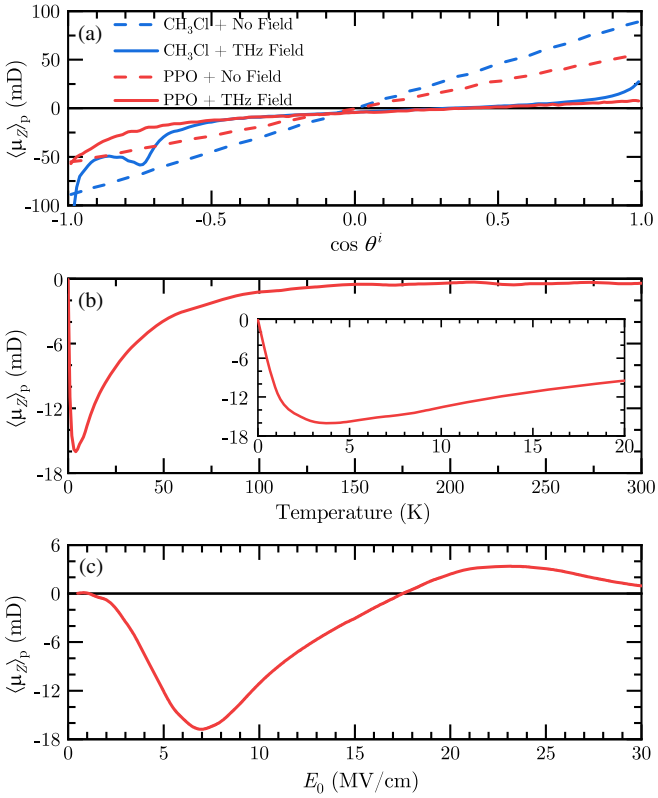

FIG. 4. (a) Classically calculated permanent values of $\langle \mu_Z \rangle_p$ as a function of initial angular position $\cos\theta^i$ for four cases: CH_3Cl without field (dashed blue), CH_3Cl and THz field (solid blue), PPO without field (dashed red), and PPO and THz field (solid red). The parameters used here are the same as in Fig. 2: $T = 5$ K, $E_0 = 8.0$ MV/cm, $\kappa = 3.06$ ps^{-2}. (b) Classically calculated permanent values of $\langle \mu_Z \rangle_p$ as a function of rotational temperature for PPO molecules excited by a pulse with fixed peak amplitude $E_0 = 8.0$ MV/cm. (c) Classically calculated permanent values of $\langle \mu_Z \rangle_p$ as a function of E_0 for PPO molecules at initial rotational temperature $T = 5$ K.

It was pointed out earlier that at $T = 0$ K permanent orientation is impossible. Also, as $T \to \infty$ the orientation disappears, as well. This nonmonotonous temperature dependence leads to the existence of an optimal initial temperature that provides the maximal (in absolute value) permanent orientation. Figure 4(b) depicts the temperature dependence of the permanent dipole signal calculated classically. For the pulse parameters used here, the maximal persistent orientation is achieved for the initial temperature of $T \approx 4$ K. Clearly, the pulse amplitude affects the orientation as well. Figure 4(c) depicts the pulse amplitude dependence of the permanent orientation. It demonstrates a

nontrivial nonmonotonous behavior that has a clear physical origin. Orientation is zero for vanishing amplitudes, and it asymptotically tends to zero at extremely high amplitudes for which one may neglect the initial thermal motion of molecules. This suggests the existence of the extremum in the orientation dependence on the field strength. Note that the minimum seen in Fig. 4(c) corresponds to a realistic value for currently available THz pulses.

Summary.—We have theoretically demonstrated a new phenomenon of persistent orientation of symmetric- and asymmetric-top molecules excited by a single THz pulse. The orientation was shown to persist long after the end of the pulse for both types of molecules. Analysis of the relatively simple special case of symmetric-top molecules reveals the underlying classical mechanism and provides a detailed understanding. The mechanism is general and relies on the symmetry breaking of the molecular ensemble caused by the interaction with the external field. A similar mechanism may lead to a persistent orientation effect in the cases of symmetric and asymmetric tops excited by two-color laser fields [44–48]. The fast transient dipole signal and its long-time persistent component may be directly measured with the help of second (or higher order) harmonic generation, which is sensitive to the lack of inversion symmetry [47]. The existence of long term orientation may open up possibilities for further molecular control and to deflection of the excited molecules by inhomogeneous electrostatic fields. Thus, one can envisage selective excitation of specific molecules in a mixture followed by selective deflection of the excited molecules, giving rise to separation of various species in a gaseous mixture.

This work was supported by the Israel Science Foundation (Grant No. 746/15), the ISF-NSFC joint research program (Grant No. 2520/17). I. A. acknowledges support as the Patricia Elman Bildner Professorial Chair. This research was made possible in part by the historic generosity of the Harold Perlman Family.

L. X. and I. T. contributed equally to this work.

*ilya.averbukh@weizmann.ac.il

[1] H. Stapelfeldt and T. Seideman, Colloquium: Aligning molecules with strong laser pulses, Rev. Mod. Phys. **75**, 543 (2003).

[2] Y. Ohshima and H. Hasegawa, Coherent rotational excitation by intense nonresonant laser fields, Int. Rev. Phys. Chem. **29**, 619 (2010).

[3] S. Fleischer, Y. Khodorkovsky, E. Gershnabel, Y. Prior, and I. Sh. Averbukh, Molecular alignment induced by ultrashort laser pulses and its impact on molecular motion, Isr. J. Chem. **52**, 414 (2012).

[4] M. Lemeshko, R. V. Krems, J. M. Doyle, and S. Kais, Manipulation of molecules with electromagnetic fields, Mol. Phys. **111**, 1648 (2013).

[5] C. P. Koch, M. Lemeshko, and D. Sugny, Quantum control of molecular rotation, Rev. Mod. Phys. **91**, 035005 (2019).

[6] K.-L. Yeh, M. C. Hoffmann, J. Hebling, and K. A. Nelson, Generation of 10 μJ ultrashort terahertz pulses by optical rectification, Appl. Phys. Lett. **90**, 171121 (2007).

[7] S. Fleischer, Y. Zhou, R. W. Field, and K. A. Nelson, Molecular Orientation and Alignment by Intense Single-Cycle THz Pulses, Phys. Rev. Lett. **107**, 163603 (2011).

[8] K. Kitano, N. Ishii, N. Kanda, Y. Matsumoto, T. Kanai, M. Kuwata-Gonokami, and J. Itatani, Orientation of jet-cooled polar molecules with an intense single-cycle THz pulse, Phys. Rev. A **88**, 061405(R) (2013).

[9] K. N. Egodapitiya, S. Li, and R. R. Jones, Terahertz-Induced Field-Free Orientation of Rotationally Excited Molecules, Phys. Rev. Lett. **112**, 103002 (2014).

[10] P. Babilotte, K. Hamraoui, F. Billard, E. Hertz, B. Lavorel, O. Faucher, and D. Sugny, Observation of the field-free orientation of a symmetric-top molecule by terahertz laser pulses at high temperature, Phys. Rev. A **94**, 043403 (2016).

[11] R. Damari, S. Kallush, and S. Fleischer, Rotational Control of Asymmetric Molecules: Dipole-Versus Polarizability-Driven Rotational Dynamics, Phys. Rev. Lett. **117**, 103001 (2016).

[12] O. Atabek, C. M. Dion, and A. B. H. Yedder, Evolutionary algorithms for the optimal laser control of molecular orientation, J. Phys. B **36**, 4667 (2003).

[13] D. Daems, S. Guérin, D. Sugny, and H. R. Jauslin, Efficient and Long-Lived Field-Free Orientation of Molecules by a Single Hybrid Short Pulse, Phys. Rev. Lett. **94**, 153003 (2005).

[14] E. Gershnabel, I. Sh. Averbukh, and R. J. Gordon, Orientation of molecules via laser-induced antialignment, Phys. Rev. A **73**, 061401(R) (2006).

[15] K. Kitano, N. Ishii, and J. Itatani, High degree of molecular orientation by a combination of THz and femtosecond laser pulses, Phys. Rev. A **84**, 053408 (2011).

[16] C.-C. Shu and N. E. Henriksen, Field-free molecular orientation induced by single-cycle THz pulses: The role of resonance and quantum interference, Phys. Rev. A **87**, 013408 (2013).

[17] M. Yoshida and Y. Ohtsuki, Control of molecular orientation with combined near-single-cycle THz and optimally designed non-resonant laser pulses: Carrier-envelope phase effects, Chem. Phys. Lett. **633**, 169 (2015).

[18] M. Mirahmadi, B. Schmidt, M. Karra, and B. Friedrich, Dynamics of polar polarizable rotors acted upon by unipolar electromagnetic pulses: From the sudden to the adiabatic regime, J. Chem. Phys. **149**, 174109 (2018).

[19] P. M. Felker, Rotational coherence spectroscopy: Studies of the geometries of large gas-phase species by picosecond time-domain methods, J. Phys. Chem. **96**, 7844 (1992).

[20] I. Sh. Averbukh and N. F. Perelman, Fractional revivals: Universality in the long-term evolution of quantum wave packets beyond the correspondence principle dynamics, Phys. Lett. A **139**, 449 (1989).

[21] R. W. Robinett, Quantum wave packet revivals, Phys. Rep. **392**, 1 (2004).

[22] C. A. Arango and G. S. Ezra, Classical mechanics of dipolar asymmetric top molecules in collinear static electric and

nonresonant linearly polarized laser fields: Energy-momentum diagrams, bifurcations and accessible configuration space, Int. J. Bifurcation Chaos Appl. Sci. Eng. **18**, 1127 (2008).

[23] K. Schatz, B. Friedrich, S. Becker, and B. Schmidt, Symmetric tops in combined electric fields: Conditional quasisolvability via the quantum Hamilton-Jacobi theory, Phys. Rev. A **97**, 053417 (2018).

[24] R. V. Krems, *Molecules in Electromagnetic Fields: From Ultracold Physics to Controlled Chemistry* (Wiley, New York, 2018).

[25] L. H. Coudert, Optimal orientation of an asymmetric top molecule with terahertz pulses, J. Chem. Phys. **146**, 024303 (2017).

[26] M. Clerici, M. Peccianti, B. E. Schmidt, L. Caspani, M. Shalaby, M. Giguère, A. Lotti, A. Couairon, F. Légaré, T. Ozaki, D. Faccio, and R. Morandotti, Wavelength Scaling of Terahertz Generation by Gas Ionization, Phys. Rev. Lett. **110**, 253901 (2013).

[27] T. I. Oh, Y. J. Yoo, Y. S. You, and K. Y. Kim, Generation of strong terahertz fields exceeding 8 MV/cm at 1 kHz and real-time beam profiling, Appl. Phys. Lett. **105**, 041103 (2014).

[28] C. Vicario, A. V. Ovchinnikov, S. I. Ashitkov, M. B. Agranat, V. E. Fortov, and C. P. Hauri, Generation of 0.9-mJ THz pulses in DSTMS pumped by a $Cr:Mg_2SiO_4$ laser, Opt. Lett. **39**, 6632 (2014).

[29] M. Shalaby and C. P. Hauri, Demonstration of a low-frequency three-dimensional terahertz bullet with extreme brightness, Nat. Commun. **6**, 5976 (2015).

[30] R. N. Zare, *Angular Momentum: Understanding Spatial Aspects in Chemistry and Physics* (Wiley, New York, 1988).

[31] R. B. Sidje, ExpoKit: A software package for computing matrix exponentials, ACM Trans. Math. Softw. **24**, 130 (1998).

[32] R. S. McDowell, Rotational partition functions for symmetric-top molecules, J. Chem. Phys. **93**, 2801 (1990).

[33] See Supplemental Material at http://link.aps.org/supplemental/10.1103/PhysRevLett.125.013201 for further details on the simulations (Sec. I), for the molecular properties of two molecules, methyl chloride and propylene oxide (Sec. II), for the effect of centrifugal distortion in the case of symmetric top molecule (Sec. III), for the motion of a free symmetric-top molecule (Sec. IV), as well as for a model system of symmetric-top molecules in a constant dc field (Sec. V), which includes Refs. [24,25,30,32,34,35].

[34] M. J. Frisch, G. W. Trucks, H. B. Schlegel, G. E. Scuseria, M. A. Robb, J. R. Cheeseman, G. Scalmani, V. Barone, G. A. Petersson, H. Nakatsuji *et al.*, *Gaussian 16 Revision A. 03* (Gaussian Inc., Wallingford CT, 2016).

[35] G. M. Black and M. M. Law, The general harmonic force field of methyl chloride, J. Mol. Spectrosc. **205**, 280 (2001).

[36] H. Goldstein, C. Poole, and J. Safko, *Classical Mechanics* (Addison Wesley, San Francisco, CA, 2002).

[37] E. A. Coutsias and L. Romero, The quaternions with an application to rigid body dynamics, Sandia Technical Report No. SAND2004-0153, 2004.

[38] J. B. Kuipers, *Quaternions and Rotation Sequences: A Primer with Applications to Orbits, Aerospace and Virtual Reality* (Princeton University Press, Princeton, N.J., 1999).

[39] S. M. LaValle, *Planning Algorithms* (Cambridge University Press, New York, 2006).

[40] S. Keshavamurthy and P. Schlagheck, *Dynamical Tunneling: Theory and Experiment* (CRC Press, Boca Raton, 2011).

[41] R. Damari, D. Rosenberg, and S. Fleischer, Coherent Radiative Decay of Molecular Rotations: A Comparative Study of Terahertz-Oriented Versus Optically Aligned Molecular Ensembles, Phys. Rev. Lett. **119**, 033002 (2017).

[42] I. Tutunnikov, J. Floß, E. Gershnabel, P. Brumer, and I. Sh. Averbukh, Laser-induced persistent orientation of chiral molecules, Phys. Rev. A **100**, 043406 (2019).

[43] I. Tutunnikov, J. Floß, E. Gershnabel, P. Brumer, I. Sh. Averbukh, A. A. Milner, and V. Milner, Observation of persistent orientation of chiral molecules by a laser field with twisted polarization, Phys. Rev. A **101**, 021403(R) (2020).

[44] S. De, I. Znakovskaya, D. Ray, F. Anis, N. G. Johnson, I. A. Bocharova, M. Magrakvelidze, B. D. Esry, C. L. Cocke, I. V. Litvinyuk, and M. F. Kling, Field-Free Orientation of CO Molecules by Femtosecond Two-Color Laser Fields, Phys. Rev. Lett. **103**, 153002 (2009).

[45] K. Oda, M. Hita, S. Minemoto, and H. Sakai, All-Optical Molecular Orientation, Phys. Rev. Lett. **104**, 213901 (2010).

[46] J. Wu and H. Zeng, Field-free molecular orientation control by two ultrashort dual-color laser pulses, Phys. Rev. A **81**, 053401 (2010).

[47] E. Frumker, C. T. Hebeisen, N. Kajumba, J. B. Bertrand, H. J. Wörner, M. Spanner, D. M. Villeneuve, A. Naumov, and P. B. Corkum, Oriented Rotational Wave-Packet Dynamics Studies Via High Harmonic Generation, Phys. Rev. Lett. **109**, 113901 (2012).

[48] K. Lin, I. Tutunnikov, J. Qiang, J. Ma, Q. Song, Q. Ji, W. Zhang, H. Li, F. Sun, X. Gong, H. Li, P. Lu, H. Zeng, Y. Prior, I. Sh. Averbukh, and J. Wu, All-optical field-free three-dimensional orientation of asymmetric-top molecules, Nat. Commun. **9**, 5134 (2018).